Stability Performance of Power Electronic Devices with Time Delays

Uros Markovic*, Petros Aristidou§, Gabriela Hug*
* EEH - Power Systems Laboratory, ETH Zurich, Physikstrasse 3, 8092 Zurich, Switzerland
§ School of Electronic and Electrical Engineering, University of Leeds, Leeds LS2 9JT, UK
Emails: {markovic, hug}@eeh.ee.ethz.ch, p.aristidou@leeds.ac.uk

***Abstract*—This paper deals with the impact of time delays on small-signal stability of power systems with an all converter-interfaced generation. For this purpose, a delay differential algebraic equation model of the voltage source converter and its control scheme is developed. The regulation is based on replicating the dynamical properties of a synchronous machine through appropriate controller configuration. Therefore, a virtual inertia emulation is included in the active power control loop. A transcedental nature of the characteristic equation is resolved by implementing the Chebyshev's discretization method and observing a finite number of critical, low-frequency eigenvalues. Based on the proposed approach, a critical measurement delay is evaluated. Furthermore, a bifurcation analysis of the droop gains and inertia constant is conducted. Stability regions and optimal parametrization of the voltage source converter controls are evaluated and discussed.**

***Index Terms*—voltage source converter (VSC), delay differential algebraic equations (DDAE), small-signal stability, low-inertia systems**

I. Introduction

The share of Power Electronic (PE) devices in power systems is growing rapidly, as the major transition from large synchronous machines to smaller, PE-interfaced, Distributed Generators (DGs) is occurring. This transformation is accompanied by a loss of rotational inertia and leads to so-called low-inertia systems with some adverse effects on the system stability margins [1]. To compensate for this, some alternative converter control concepts, mainly based on virtual inertia emulation, have been proposed in literature [2]–[5], trying to reproduce the stabilizing effects provided by naturally occurring inertia in conventional power systems. Despite employing different regulation strategies, all of the suggested methods imply replicating the dynamical characteristics of a synchronous machine through adequate Voltage Source Converter (VSC) operation schemes.

When analyzing the stability of these low-inertia systems, the correct modeling of PE-interfaced devices and their controllers is of crucial importance for extracting meaningful information. One of the most widely used methods for analyzing power system stability is with small-signal analysis which provides useful information on the system stability and oscillatory modes. A small-signal analysis of a low-inertia system has been conducted in [6]. However, the impact of time delays coming from measurement or communication in the PE components has not been included, which can play an important role in system stability. The work in [7] takes into account signal delays in a system with 100% DG penetration, but only in the form of a simplified Padé approximant, which might lead to inaccurate results and is computationally intensive [8]. A probabilistic approach to evaluate the small-signal stability of power systems in the presence of communication delays is presented in [9], by modeling the delay margin as a random variable and employing Monte Carlo simulations. Nevertheless, it is applied only to a Single-Machine Infinite-Bus (SMIB) system with an exciter. A similar SMIB model is studied in [10], which reduces the problem complexity and enables its observation through a set of Delayed Differential Equations (DDEs). It concludes that the small delays can be ignored, while the larger ones could significantly change the dynamic characteristics of the system.

In order to properly analyze the stability properties of power systems taking into account signal delays, their conventional mathematical representation, based on Differential Algebraic Equations (DAEs), must be extended to Delay Differential Algebraic Equations (DDAEs). The variations of this concept have been investigated in [11], but only for the case of a synchronous machine with signal delays in the terminal voltage measurement, as well as the respective transducers of automatic voltage regulators and power system stabilizers. Additionally, the study in [12] has confirmed the impact of large measurement delays on the boundary of the small signal stability region via a "predictor–corrector" framework, employing an optimization problem as the algorithm's corrector. The downside of the proposed approach is the imprecise time delay approximation, as well as the validation for only simple power systems.

The contribution of this work is two-fold. First, we introduce a VSC model with a state-of-the-art control structure including virtual inertia emulation. Then, a DDAE set of the investigated system is derived for the purposes of small-signal analysis. Second, the critical eigenvalues of the system are determined using the Chebyshev's discretization method and adequate stability margins are assessed based on bifurcation analysis.

This project has received funding from the *European Union's Horizon 2020 research and innovation programme* under grant agreement No 691800. This paper reflects only the authors' views and the European Commission is not responsible for any use that may be made of the information it contains.

Furthermore, the properties of the employed interpolation scheme are investigated.

The remainder of the paper is structured as follows. In Section II, the small-signal stability of delayed power systems is introduced. Section III describes the proposed model of the VSC control scheme and its DDAE formulation. Section IV showcases the results of the eigenvalue and bifurcation analysis, whereas Section V offers some concluding remarks.

II. Small-Signal Analysis of DDAE

A. General DDAE Form for Power Systems

The dynamic behavior of electric power systems is usually described with a set of DAEs as follows [11], [13]:

$$\begin{aligned} \dot{\boldsymbol{x}} &= \boldsymbol{f}(\boldsymbol{x}, \boldsymbol{y}, \boldsymbol{z}) \\ \boldsymbol{0} &= \boldsymbol{g}(\boldsymbol{x}, \boldsymbol{y}, \boldsymbol{z}) \end{aligned} \tag{1}$$

where $\boldsymbol{f}$ ($\boldsymbol{f} : \mathbb{R}^n \mapsto \mathbb{R}^n$) and $\boldsymbol{g}$ ($\boldsymbol{g} : \mathbb{R}^m \mapsto \mathbb{R}^m$) are respectively sets of differential and algebraic equations, $\boldsymbol{x}$ ($\boldsymbol{x} \in \mathbb{R}^n$) and $\boldsymbol{y}$ ($\boldsymbol{y} \in \mathbb{R}^m$) are respectively vectors of the state and algebraic variables, and $\boldsymbol{z}$ ($\boldsymbol{z} \in \mathbb{R}^k$) is a vector of the discrete event variables. Despite being widely used in power system studies, system (1) fails to capture accurately the time delays and their potential impact on the overall system stability. In most investigations, time delays are either neglected or represented by first order models. The proper introduction of time delays transforms the DAE model into a set of DDAEs. Assuming a single constant time delay $\tau > 0$ affecting the measurements, the delayed vectors of state ($\boldsymbol{x}_\tau$) and algebraic ($\boldsymbol{y}_\tau$) variables can be defined as:

$$\begin{aligned} \boldsymbol{x}_\tau &= \boldsymbol{x}(t-\tau) \\ \boldsymbol{y}_\tau &= \boldsymbol{y}(t-\tau) \end{aligned} \tag{2}$$

with t denoting the current simulation time. The general form of DDAE can be further simplified for practical models of power systems, by reducing the actual set of delayed equations to the index-1 Hessenberg form, as described in [14]:

$$\begin{aligned} \dot{\boldsymbol{x}} &= \boldsymbol{f}(\boldsymbol{x}, \boldsymbol{y}, \boldsymbol{x}_\tau, \boldsymbol{y}_\tau, \boldsymbol{z}) \\ \boldsymbol{0} &= \boldsymbol{g}(\boldsymbol{x}, \boldsymbol{y}, \boldsymbol{x}_\tau, \boldsymbol{z}) \end{aligned} \tag{3}$$

In other words, it is assumed that $\boldsymbol{g}$ does not depend on $\boldsymbol{y}_\tau$. However, there is no loss of generality between (3) and the initial system model [11].

B. Characteristic Equation of General DDAE

Let us assume a known stationary solution $(\boldsymbol{x}_0, \boldsymbol{y}_0)$ of (3):

$$\begin{aligned} \boldsymbol{0} &= \boldsymbol{f}(\boldsymbol{x}_0, \boldsymbol{y}_0, \boldsymbol{x}_0, \boldsymbol{y}_0, \boldsymbol{z}_0) \\ \boldsymbol{0} &= \boldsymbol{g}(\boldsymbol{x}_0, \boldsymbol{y}_0, \boldsymbol{x}_0, \boldsymbol{z}_0) \end{aligned} \tag{4}$$

By linearizing the respective set of DDAE at the stationary point one can obtain the following expression:

$$\Delta\dot{\boldsymbol{x}} = \boldsymbol{f}_{\boldsymbol{x}}\Delta\boldsymbol{x} + \boldsymbol{f}_{\boldsymbol{x}_\tau}\Delta\boldsymbol{x}_\tau + \boldsymbol{f}_{\boldsymbol{y}}\Delta\boldsymbol{y} + \boldsymbol{f}_{\boldsymbol{y}_\tau}\Delta\boldsymbol{y}_\tau \tag{5}$$

$$\boldsymbol{0} = \boldsymbol{g}_{\boldsymbol{x}}\Delta\boldsymbol{x} + \boldsymbol{g}_{\boldsymbol{x}_\tau}\Delta\boldsymbol{x}_\tau + \boldsymbol{g}_{\boldsymbol{y}}\Delta\boldsymbol{y} \tag{6}$$

which can be further simplified by deriving $\Delta\boldsymbol{y}$ from (6) and substituting it in (5):

$$\begin{aligned} \Delta\boldsymbol{y} =& -\boldsymbol{g}_{\boldsymbol{y}}^{-1}\boldsymbol{g}_{\boldsymbol{x}}\Delta\boldsymbol{x} - \boldsymbol{g}_{\boldsymbol{y}}^{-1}\boldsymbol{g}_{\boldsymbol{x}_\tau}\Delta\boldsymbol{x}_\tau \overset{(5)}{\longmapsto} \\ \Delta\dot{\boldsymbol{x}} =& \boldsymbol{f}_{\boldsymbol{x}}\Delta\boldsymbol{x} + \boldsymbol{f}_{\boldsymbol{x}_\tau}\Delta\boldsymbol{x}_\tau - \boldsymbol{f}_{\boldsymbol{y}}\left(\boldsymbol{g}_{\boldsymbol{y}}^{-1}\boldsymbol{g}_{\boldsymbol{x}}\Delta\boldsymbol{x}\right) - \\ & \boldsymbol{f}_{\boldsymbol{y}}\left(\boldsymbol{g}_{\boldsymbol{y}}^{-1}\boldsymbol{g}_{\boldsymbol{x}_\tau}\Delta\boldsymbol{x}_\tau\right) + \boldsymbol{f}_{\boldsymbol{y}_\tau}\Delta\boldsymbol{y}_\tau \end{aligned} \tag{7}$$

Hence, the final form of $\Delta\dot{\boldsymbol{x}}$ yields:

$$\begin{aligned} \Delta\dot{\boldsymbol{x}} =& \left(\boldsymbol{f}_{\boldsymbol{x}} - \boldsymbol{f}_{\boldsymbol{y}}\boldsymbol{g}_{\boldsymbol{y}}^{-1}\boldsymbol{g}_{\boldsymbol{x}}\right)\Delta\boldsymbol{x} + \\ & \left(\boldsymbol{f}_{\boldsymbol{x}_\tau} - \boldsymbol{f}_{\boldsymbol{y}}\boldsymbol{g}_{\boldsymbol{y}}^{-1}\boldsymbol{g}_{\boldsymbol{x}_\tau}\right)\Delta\boldsymbol{x}_\tau + \\ & \boldsymbol{f}_{\boldsymbol{y}_\tau}\Delta\boldsymbol{y}_\tau \end{aligned} \tag{8}$$

Understandably, a usual assumption of a non-singular characteristic of $\boldsymbol{g}_{\boldsymbol{y}}$ must be made in order to make (8) feasible. Furthermore, a substitution of the $\Delta\boldsymbol{y}_\tau$ vector with a linear form of the actual or delayed state variables is necessary to achieve a meaningful expression. This is done by considering the set of algebraic equations $\boldsymbol{g}$ at time step $(t-\tau)$:

$$\boldsymbol{0} = \boldsymbol{g}(\boldsymbol{x}(t-\tau), \boldsymbol{y}(t-\tau), \boldsymbol{x}_\tau(t-\tau)) \tag{9}$$

Since the following equalities hold

$$\boldsymbol{x}_\tau = \boldsymbol{x}(t-\tau);\ \ \boldsymbol{y}_\tau = \boldsymbol{y}(t-\tau);\ \ \boldsymbol{x}_\tau(t-\tau) = \boldsymbol{x}(t-2\tau) \tag{10}$$

it is possible to differentiate (9), resulting in

$$\boldsymbol{0} = \boldsymbol{g}_{\boldsymbol{x}}\Delta\boldsymbol{x}_\tau + \boldsymbol{g}_{\boldsymbol{y}}\Delta\boldsymbol{y}_\tau + \boldsymbol{g}_{\boldsymbol{x}_\tau}\Delta\boldsymbol{x}(t-2\tau) \tag{11}$$

This work focuses only on simple systems where it can be justifiably assumed that only one type of time delay is present in the model (see Eq. 2). The explanation for this is that delayed variables correspond to measurement delays, which can be expected to be very similar for different devices. Therefore, we can simplify (11) by eliminating its last term:

$$\boldsymbol{0} = \boldsymbol{g}_{\boldsymbol{x}}\Delta\boldsymbol{x}_\tau + \boldsymbol{g}_{\boldsymbol{y}}\Delta\boldsymbol{y}_\tau \tag{12}$$

It should be noted that the Jacobian matrices in (6) and (12) are the same, since variables $\boldsymbol{x}$ and $\boldsymbol{y}$ meet the following steady state conditions at any instance t_0:

$$\boldsymbol{x}(t_0) = \boldsymbol{x}(t_0-\tau);\ \ \boldsymbol{y}(t_0) = \boldsymbol{y}(t_0-\tau) \tag{13}$$

Similar to the mathematical transformation in (7), we can now derive $\Delta\boldsymbol{y}_\tau$ from (12) and substitute it in (8), which yields:

$$\begin{aligned} \Delta\boldsymbol{y}_\tau =& -\boldsymbol{g}_{\boldsymbol{y}}^{-1}\boldsymbol{g}_{\boldsymbol{x}}\Delta\boldsymbol{x}_\tau \overset{(8)}{\longmapsto} \\ \Delta\dot{\boldsymbol{x}} =& \left(\boldsymbol{f}_{\boldsymbol{x}} - \boldsymbol{f}_{\boldsymbol{y}}\boldsymbol{g}_{\boldsymbol{y}}^{-1}\boldsymbol{g}_{\boldsymbol{x}}\right)\Delta\boldsymbol{x} + \\ & \left(\boldsymbol{f}_{\boldsymbol{x}_\tau} - \boldsymbol{f}_{\boldsymbol{y}}\boldsymbol{g}_{\boldsymbol{y}}^{-1}\boldsymbol{g}_{\boldsymbol{x}_\tau} - \boldsymbol{f}_{\boldsymbol{y}_\tau}\boldsymbol{g}_{\boldsymbol{y}}^{-1}\boldsymbol{g}_{\boldsymbol{x}}\right)\Delta\boldsymbol{x}_\tau \end{aligned} \tag{14}$$

The final form of (14) can be declared as:

$$\Delta\dot{\boldsymbol{x}} = \boldsymbol{A}_0\Delta\boldsymbol{x} + \boldsymbol{A}_1\Delta\boldsymbol{x}(t-\tau) \tag{15}$$

where,

$$\boldsymbol{A}_0 = \boldsymbol{f}_{\boldsymbol{x}} - \boldsymbol{f}_{\boldsymbol{y}}{\boldsymbol{g}_{\boldsymbol{y}}}^{-1}\boldsymbol{g}_{\boldsymbol{x}} \tag{16}$$

$$\boldsymbol{A}_1 = \boldsymbol{f}_{\boldsymbol{x}_\tau} - \boldsymbol{f}_{\boldsymbol{y}}{\boldsymbol{g}_{\boldsymbol{y}}}^{-1}\boldsymbol{g}_{\boldsymbol{x}_\tau} - \boldsymbol{f}_{\boldsymbol{y}_\tau}{\boldsymbol{g}_{\boldsymbol{y}}}^{-1}\boldsymbol{g}_{\boldsymbol{x}} \tag{17}$$

Equation (16) denotes a standard DAE state matrix $\boldsymbol{A}_0$, whereas $\boldsymbol{A}_1$ is a consequence of the time delays. The formulation in (15) represents a special case of the standard DDE form:

$$\dot{\boldsymbol{x}} = \boldsymbol{A}_0\boldsymbol{x}(t) + \sum_{i=1}^{\nu} \boldsymbol{A}_i\boldsymbol{x}_i(t-\tau_i) \tag{18}$$

whose characteristic matrix can be defined as:

$$\Delta(\lambda) = \lambda\boldsymbol{I}_n - \boldsymbol{A}_0 - \sum_{i=1}^{\nu} \boldsymbol{A}_i e^{-\lambda\tau_i} \tag{19}$$

The matrix $\boldsymbol{I}_n$ is the identity matrix of order n, while in this specific case, $\nu = 1$ and $\tau_1 = \tau$. Despite (19) being transcedental, the number of its right-half plane solutions is finite and, therefore, can be used for small-signal stability studies [15]. Furthermore, the stability properties of the respective root spectrum are applicable to the DDAE system in (15). More details regarding the derivation of expressions (15)-(19) for multiple-delay systems, as well as the theoretical background behind the eigenvalue properties of (19), can be found in [11].

C. Solution Approximation Technique

Since the explicit solution of (19) is not known, certain numerical approximations have to be employed in order to find a finite subset of the initial roots which reflect the same stability characteristics. The study in [8] analyzed four different approaches that approximate the solution of the small-signal stability of DDAE, and concluded that the Chebyshev's discretization scheme proposed in [16]–[18] is the most accurate and robust method. This technique is based on recasting (18) as an abstract Cauchy problem, i.e. transforming the initial eigenvalue analysis of a DDE system into computing roots of an infinite dimensional set of Partial Differential Equations (PDE), without any loss of information. Subsequently, a finite element-based discretization method is employed in order to make PDE problem computations tractable.

For the purposes of our study, a simplification that only state variables are subjected to time delays can be made. In other words, by assuming a single event variable, we can reformulate (3) into:

$$\begin{aligned} \dot{\boldsymbol{x}} &= \boldsymbol{f}(\boldsymbol{x},\, \boldsymbol{y},\, \boldsymbol{x}_\tau) \\ \boldsymbol{0} &= \boldsymbol{g}(\boldsymbol{x},\, \boldsymbol{y}, \boldsymbol{x}_\tau) \end{aligned} \tag{20}$$

for which the characteristic matrix becomes:

$$\Delta(\lambda) = \lambda\boldsymbol{I}_n - \boldsymbol{A}_0 - \boldsymbol{A}_1 e^{-\lambda\tau} \tag{21}$$

with,

$$\boldsymbol{A}_0 = \boldsymbol{f}_{\boldsymbol{x}} - \boldsymbol{f}_{\boldsymbol{y}}{\boldsymbol{g}_{\boldsymbol{y}}}^{-1}\boldsymbol{g}_{\boldsymbol{x}} \tag{22}$$

$$\boldsymbol{A}_1 = \boldsymbol{f}_{\boldsymbol{x}_\tau} - \boldsymbol{f}_{\boldsymbol{y}}{\boldsymbol{g}_{\boldsymbol{y}}}^{-1}\boldsymbol{g}_{\boldsymbol{x}_\tau} \tag{23}$$

The spectrum of (21) can be approximated by the eigenvalues of the discretization matrix $\boldsymbol{M}$ [8]:

$$\boldsymbol{M} = \left[\begin{array}{ccccc} \hat{\boldsymbol{C}} \otimes \boldsymbol{I}_n & & & & \\ \hline \boldsymbol{A}_1 & \boldsymbol{0} & \dots & \boldsymbol{0} & \boldsymbol{A}_0 \end{array}\right] \tag{24}$$

where $\otimes$ denotes the Kronecker product and $\hat{\boldsymbol{C}}$ indicates a matrix composed of the first $N-1$ rows of the following matrix $\boldsymbol{C}$:

$$\boldsymbol{C} = -\frac{2\boldsymbol{D}_N}{\tau} \tag{25}$$

Here, $\boldsymbol{D}_N$ represents the Chebyshev's differentiation matrix of order N, which is in fact a square matrix of dimension $(N+1)$. In order to form $\boldsymbol{D}_N$, one has to first define $(N+1)$ Chebyshev's nodes. They represent the interpolation points on the normalized interval $[-1,\, 1]$ and are structured as follows:

$$x_k = \cos\left(\frac{k\pi}{N}\right), \quad k = 0,\, \dots,\, N \tag{26}$$

Subsequently, each element $(i,\, j)$ of the differentiation matrix $\boldsymbol{D}_N$, with indices ranging from 0 to N, can be defined according to the interpolation scheme presented below:

$$\boldsymbol{D}_{(i,j)} = \begin{cases} \frac{c_i(-1)^{i+j}}{c_j(x_i - x_j)}, & i \neq j \\ \frac{-1}{2}\frac{x_i}{1-x_i^2}, & i = j \neq 1,\, N-1 \\ \frac{2N^2+1}{6}, & i = j = 0 \\ -\frac{2N^2+1}{6}, & i = j = N \end{cases}$$

where $c_0 = c_N = 2$ and $c_2 = c_3 = \ldots = c_{N-1} = 1$.

It can be seen that the selection of the number of nodes N defines the computational effort and the precision of the proposed method. Therefore, the selection of N and its impact on the overall results will be thoroughly investigated. The logic behind approximating the spectrum of (21) with the eigenvalues of $\boldsymbol{M}$ lies in considering $\boldsymbol{M}$ as a discretization of a PDE system, where a continuous variable corresponds to the time delay that is discretized along the grid of N points. The position of these points is defined by Chebyshev's polynomial interpolation, with the last n rows corresponding to the PDE boundary conditions [11].

III. Power System Modeling

In order to study the impact of time delays on the stability of the VSC controls, a simple 2-bus test system is considered, consisting of a VSC at one node and an inductive load at the other. The VSC is connected to the grid through an RC filter, while the transmission line (R_t, L_t) and the load (R_l, L_l) are both modeled as a resistor and an inductor in series.

The converter represents an interface between two different variable domains: (i) the control side in the phasor domain; and (ii) the grid side in the ElectroMagnetic Transient (EMT) domain[1]. Therefore, the VSC control can be implemented in a decoupled fashion, while simultaneously capturing dynamics of the grid components, as shown in Fig. 1.

A. VSC Control Scheme

The employed control scheme is simplified for the purpose of small-signal analysis of the DDAE. This is achieved by neglecting the standard cascade control consisting of an outer

[1]All EMT variables are denoted with the ˆ symbol.

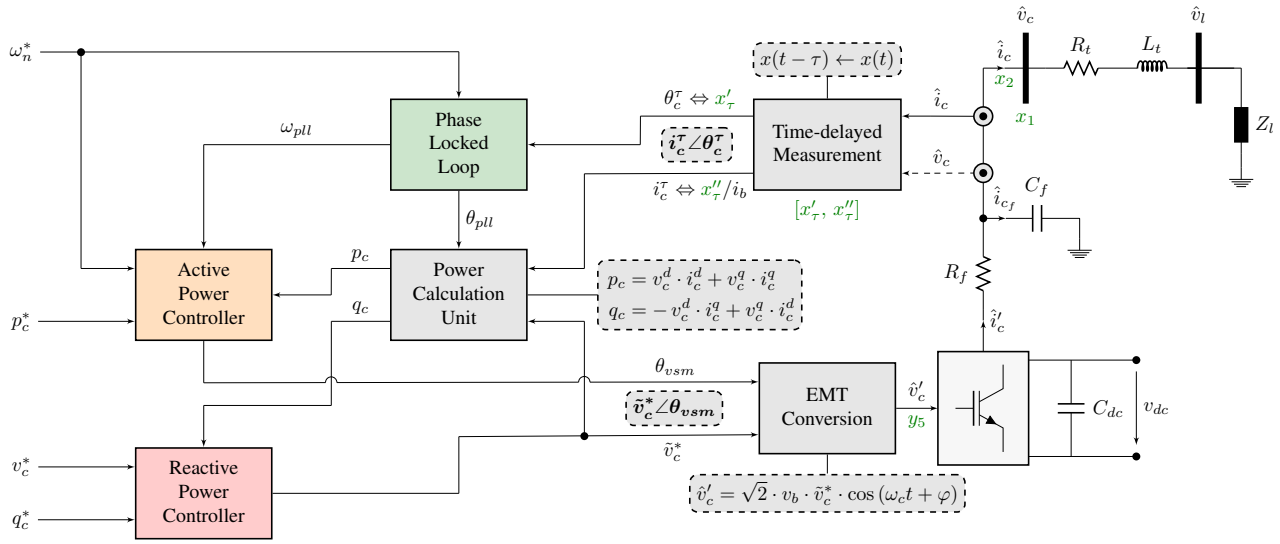

Fig. 1: Investigated system configuration and VSC control structure.

voltage and inner current control loop, together with the pulse-width modulation block [6]. In other words, the reference signals of active and reactive power controllers are computed as voltage angle (θ_{vsm}) and magnitude ($\tilde{v}_c^*$), respectively, and sent to the VSC in the EMT form of voltage $\hat{v}'_c$. Hence, the only measurement needed for signal processing of converter power components p_c and q_c is the current phasor signal $i_c^\tau \angle \theta_c^\tau$, a state variable affected by a measurement delay τ. The main control blocks are depicted in Fig. 2 and described in more detail below [6], [19].

1) Phase-Locked Loop (PLL): The PLL behaves as an observer and tracks the actual grid frequency by measuring current and passing the phase angle error through a PI control:

$$\omega_{pll} = \omega_n^* + (\theta_c^\tau - \theta_{pll}) \cdot \left(K_p + \frac{K_i}{s}\right) \tag{27}$$

The obtained frequency is then integrated in order to compute the actual phase angle θ_{pll}.

2) Active Power Controller (APC): There are several variants of the active droop control, as well as emulating the inertia [6], [19], [20]. The proposed approach is based on [6], by combining the droop control of measured frequency (D_ω) with the acceleration of virtual inertia via the power imbalance ($2H$). Additionally, a droop-like control is included to simulate the power damping of the synchronous machine (K_d):

$$\begin{aligned} 2H \cdot \dot{\omega}_{vsm} = p_c^* - p_c + D_\omega \cdot (\omega_n^* - \omega_{vsm}) + \\ K_d \cdot (\omega_{pll} - \omega_{vsm}) \end{aligned} \tag{28}$$

This control configuration provides both the conventional synchronization and the damping properties, while simultaneously regulating the active power output of the converter via an external droop loop. The outputs of the controller are the voltage angle and frequency references ($\theta_{vsm}, \omega_{vsm}$).

3) Reactive Power Controller (RPC): The reactive power controller is based on the droop control of the measured reactive power. The gain (D_q) reacts on the difference between the reactive power reference (q_c^*) and the actual power measurement (q_c). It provides the voltage magnitude reference $\tilde{v}_c^*$ for the VSC:

$$\tilde{v}_c^* = v_c^* - D_q \cdot (q_c^* - q_c) \tag{29}$$

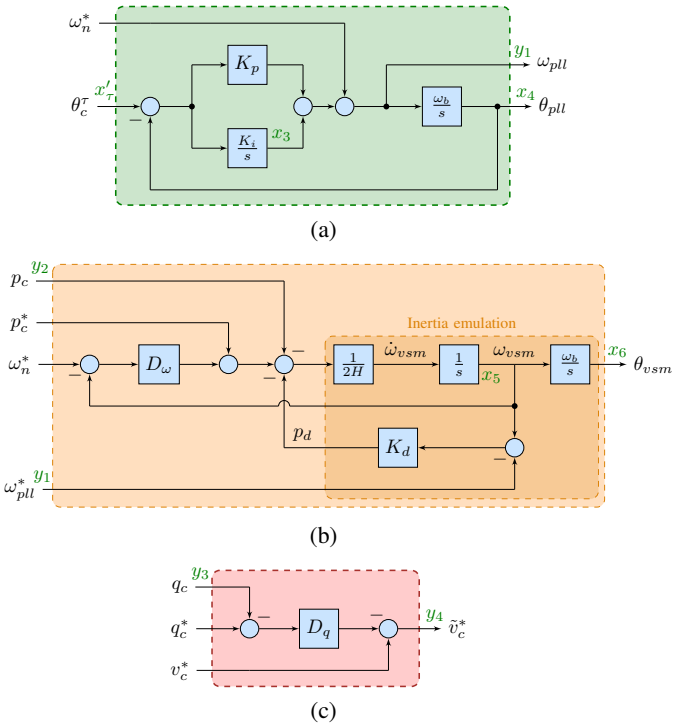

Fig. 2: Main control blocks: (a) Phase-locked loop. (b) Active power controller. (c) Reactive power controller.

B. DDAE Formulation

Based on the theory in Section II-A, a DDAE form of the proposed system is derived. The set of differential equations

can be described as:

$$\begin{aligned}
\dot{x}_1 &= \frac{1}{C_f \cdot R_f}\left(y_5 - x_1 - R_f \cdot x_2\right)\\
\dot{x}_2 &= \frac{1}{L_t + L_l} \cdot \left(x_1 - (R_t + R_l) \cdot x_2\right)\\
\dot{x}_3 &= K_i \cdot (x'_\tau - x_4)\\
\dot{x}_4 &= \omega_b \cdot y_1\\
\dot{x}_5 &= \frac{1}{2H} \cdot \left[D_\omega \cdot (\omega^*_n - x_5) + (p^*_c - y_2) - K_d \cdot (x_5 - y_1)\right]\\
\dot{x}_6 &= \omega_b \cdot x_5
\end{aligned} \tag{30}$$

whereas, the algebraic equations are formulated as follows:

$$\begin{aligned}
0 &= -y_1 + \omega^*_n + x_3 + K_p \cdot x'_\tau\\
0 &= -y_2 + y_4 \cdot \cos x_6 \cdot \frac{x''_\tau}{i_b} \cdot \cos x'_\tau + y_4 \cdot \sin x_6 \cdot \frac{x''_\tau}{i_b} \cdot \sin x'_\tau\\
0 &= -y_3 + y_4 \cdot \sin x_6 \cdot \frac{x''_\tau}{i_b} \cdot \cos x'_\tau - y_4 \cdot \cos x_6 \cdot \frac{x''_\tau}{i_b} \cdot \sin x'_\tau\\
0 &= -y_4 + v^*_c - D_q \cdot (q^*_c - y_3)\\
0 &= -y_5 + \sqrt{2} \cdot v_b \cdot y_4 \cdot \cos x_6
\end{aligned} \tag{31}$$

Parameters denoted by v_b, i_b and ω_b represent the base values of voltage, current and angular frequency, respectively. All differential ($\boldsymbol{x}$) and algebraic ($\boldsymbol{y}$) variables are defined in green color in Figs. 1 and 2.

As described previously in Section II-C, the time delay is only assumed to impact the state variables $\boldsymbol{x}_\tau = [x'_\tau, x''_\tau]^T$, and the last term in matrix $\boldsymbol{A}_1$ in (17) is set to $\boldsymbol{f}_{\boldsymbol{y}_\tau} = 0$.

IV. Results

A. Eigenvalue Spectrum Evaluation

The properties of the characteristic matrix in (19) imply that the number of its solutions in the right-half of the complex plane is finite. Hence, the small-signal stability problem of the stationary solution of (3) is reduced to the eigenvalue spectrum analysis of $\boldsymbol{M}$. Initially, the root loci of the proposed 2-bus system with measurement delay of $\tau = 100\,\text{ms}$ and $N = 5$ Chebyshev's nodes is observed and shown in Fig. 3a. We only concentrate on the eigenvalues close to the imaginary axis, i.e. the ones with low damping ratios, as they are of the interest for the small signal stability analysis. Furthermore, these rightmost solutions have small sensitivity to N, which enables us to reduce the computational burden while still maintaining the discretization accuracy [11]. This property is depicted in Fig. 3b, where the root loci of the 2-bus system for different values of N is presented. It is clear that most of the eigenvalues have very high frequency and damping factor, which makes them irrelevant for the purposes of this study. Therefore, in the remainder of the work we will solely focus on the interpolations consisting of $N = 5$ Chebyshev's nodes, in order to improve the observability of the model.

Out of the dominant eigenvalues in Fig. 3a, only a few appear to be critical having a very low damping ratio. The overall stability of the system is still preserved, which indicates that the critical delay could be well over 100 ms. Therefore,

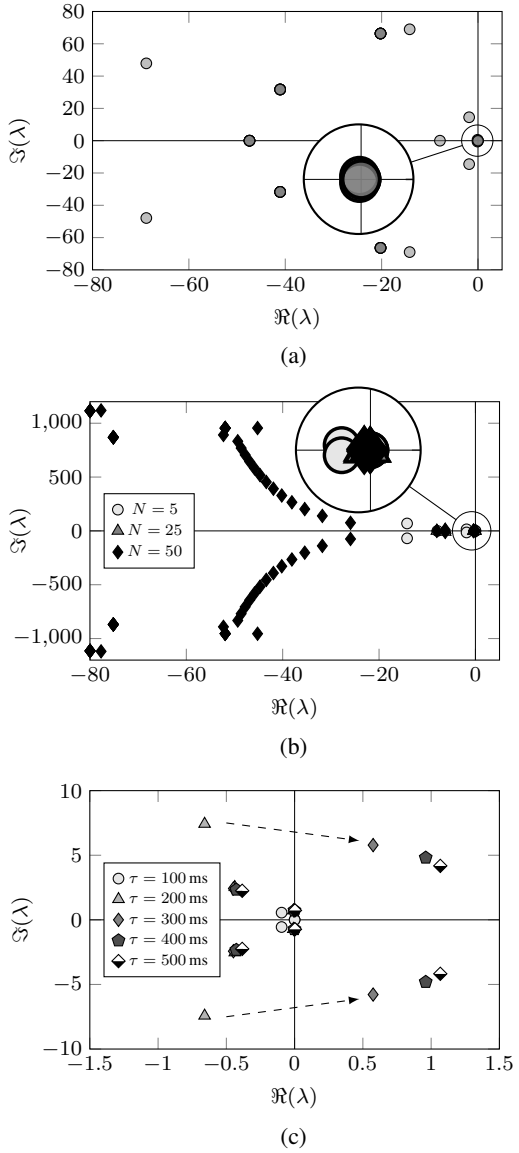

Fig. 3: Root loci of the 2-bus system: (a) Full spectrum for $N = 5$ and $\tau = 100\,\text{ms}$ (dark color indicates multiple λ). (b) Zoom close to the imaginary axis for $N \in [5, 50]$ and $\tau = 100\,\text{ms}$. (c) Zoom close to the imaginary axis for $N = 5$ and $\tau \in [100, 500]$ ms.

the measurement delay is increased in discrete steps and the movement of critical eigenvalues around the imaginary axis is tracked in Fig. 3c. The results indicate that a Hopf Bifurcation (HB) occurs for values of $\tau \in [200, 300]$ ms, more specifically $\tau = 234\,\text{ms}$. These excessive critical delay values arise due to a simplistic test system under investigation, which enables us to give insights into the effect of delays. This simple analysis is not possible in large-scale systems with multiple delays.

B. Bifurcation Analysis

For this analysis we consider varying two different groups of parameters: (i) the impact of the virtual inertia constant H on the critical time delay; and (ii) the correlation between droop

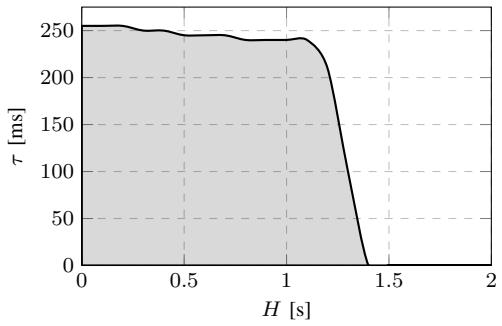

Fig. 4: Stability map on the τ-H plane. The system is stable within the shaded region.

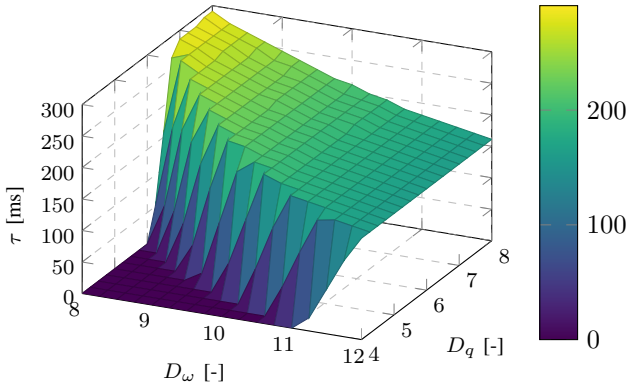

Fig. 5: Stability surface in the τ-D_ω-D_q space. The system is stable below the shaded area.

gains (D_w, D_q) and the critical time delay. The first parametric study focuses solely on the role of the artificial inertia loop within the APC. Despite improving the VSC response to power imbalances, the addition of this control loop can have an adverse effect on system stability in the presence of time delays, as confirmed by the respective stability map in Fig. 4. Assuming fast measurements ($\tau \approx 10\,\text{ms}$), the stability region is bounded by the inertia constant of $H_m \approx 1.5\,\text{s}$, whereas for $H > H_m$ the propagation of the time delay affecting the APC response leads to an unstable operation. On the other hand, the surface depicted in Fig. 5 is determined as a HB sequence for various combinations of droop gains and can be employed in deriving VSC controls by showcasing the stable (D_w, D_q) spectrum and the properties of different droop ratios under time delay. This observation approach can also provide useful insights into APC parameterization through stability surface studies in other space forms, e.g. τ-D_ω-K_d or H-D_ω-K_d.

V. Conclusion

In this paper, a small-signal stability analysis of a simple power system with PE-interfaced generation with time delays is investigated. In particular, a VSC control scheme is proposed in the index-1 Hessenberg form of DDAE and an eigenvalue analysis of the characteristic equation, obtained through the Chebyshev's discretization method, is performed. Finally, a bifurcation study of several main parameters is completed and conclusions on stability limits have been drawn with respect to control sensitivity and robustness. The impact of the employed interpolation scheme on the initial DAE solution spectrum is also analyzed. The future work will focus on more realistic systems of larger scale and the impact of time delays on the interaction between multiple converters.

References

[1] A. Ulbig, T. S. Borsche, and G. Andersson, "Impact of Low Rotational Inertia on Power System Stability and Operation," *ArXiv e-prints*, Dec. 2013.

[2] T. V. Van, K. Visscher, J. Diaz, V. Karapanos, A. Woyte, M. Albu, J. Bozelie, T. Loix, and D. Federenciuc, "Virtual synchronous generator: An element of future grids," in *2010 IEEE PES Innovative Smart Grid Technologies Conference Europe (ISGT Europe)*, Oct 2010.

[3] H. P. Beck and R. Hesse, "Virtual synchronous machine," in *2007 9th International Conference on Electrical Power Quality and Utilisation*, Oct 2007.

[4] S. D'Arco and J. A. Suul, "Virtual synchronous machines - classification of implementations and analysis of equivalence to droop controllers for microgrids," in *2013 IEEE Grenoble Conference*, June 2013.

[5] J. Driesen and K. Visscher, "Virtual synchronous generators," in *2008 IEEE Power and Energy Society General Meeting - Conversion and Delivery of Electrical Energy in the 21st Century*, July 2008.

[6] S. D'Arco, J. A. Suul, and O. B. Fosso, "Small-signal modelling and parametric sensitivity of a virtual synchronous machine," in *2014 Power Systems Computation Conference*, Aug 2014.

[7] D. Ramasubramanian, V. Vittal, and J. M. Undrill, "Transient stability analysis of an all converter interfaced generation wecc system," in *2016 Power Systems Computation Conference (PSCC)*, June 2016.

[8] F. Milano, "Small-signal stability analysis of large power systems with inclusion of multiple delays," *IEEE Transactions on Power Systems*, vol. 31, no. 4, pp. 3257–3266, July 2016.

[9] S. Ayasun and C. O. Nwankpa, "Probability of small-signal stability of power systems in the presence of communication delays," in *2009 International Conference on Electrical and Electronics Engineering - ELECO 2009*, Nov 2009.

[10] H. Jia, N. Guangyu, S. T. Lee, and P. Zhang, "Study on the impact of time delay to power system small signal stability," in *MELECON 2006 - 2006 IEEE Mediterranean Electrotechnical Conference*, May 2006.

[11] F. Milano and M. Anghel, "Impact of time delays on power system stability," *IEEE Transactions on Circuits and Systems I: Regular Papers*, vol. 59, no. 4, pp. 889–900, April 2012.

[12] H. Jia, X. Yu, Y. Yu, and C. Wang, "Power system small signal stability region with time delay," *International Journal of Electrical Power & Energy Systems*, vol. 30, no. 1, pp. 16 – 22, 2008.

[13] I. A. Hiskens, "Power system modeling for inverse problems," *IEEE Transactions on Circuits and Systems I: Regular Papers*, vol. 51, no. 3, pp. 539–551, March 2004.

[14] U. M. Ascher and L. R. Petzold, "The numerical solution of delay-differential-algebraic equations of retarded and neutral type," *SIAM Journal on Numerical Analysis*, vol. 32, no. 5, pp. 1635–1657, 1995.

[15] W. Michiels and S.-I. Niculescu, *Stability and Stabilization of Time-Delay Systems (Advances in Design & Control)*. Philadelphia, PA, USA: Society for Industrial and Applied Mathematics, 2007.

[16] A. Bellen and S. Maset, "Numerical solution of constant coefficient linear delay differential equations as abstract cauchy problems," *Numerische Mathematik*, vol. 84, no. 3, pp. 351–374, 2000.

[17] A. Bellen and M. Zennaro, *Numerical Methods for Delay Differential Equations*. Oxford: Oxford University Press, 2003.

[18] D. Breda, S. Maset, and R. Vermiglio, "Pseudospectral approximation of eigenvalues of derivative operators with non-local boundary conditions," *Applied Numerical Mathematics*, vol. 56, no. 3, pp. 318 – 331, 2006.

[19] Y. Du, J. M. Guerrero, L. Chang, J. Su, and M. Mao, "Modeling, analysis, and design of a frequency-droop-based virtual synchronous generator for microgrid applications," in *2013 IEEE ECCE Asia Downunder*, June 2013.

[20] J. Liu, Y. Miura, and T. Ise, "Comparison of dynamic characteristics between virtual synchronous generator and droop control in inverter-based distributed generators," *IEEE Transactions on Power Electronics*, vol. 31, no. 5, pp. 3600–3611, May 2016.